Check for updates

Multimodal integrated flexible neural probe for *in situ* monitoring of EEG and lactic acid

Luxi Zhang, [ID] Jie Xia, Boyu Li, Zhen Cao* and Shurong Dong [ID] *

In physiological activities, the brain's electroencephalogram (EEG) signal and chemical concentration change are crucial for diagnosing and treating neurological disorders. Despite the advantages of flexible neural probes, such as their flexibility and biocompatibility, it remains a challenge to achieve *in situ* monitoring of electrophysiological and chemical signals on a small scale simultaneously. This study developed a new method to construct an efficient dual-sided multimodal integrated flexible neural probe, which combines a density electrode array for EEG recordings and an electrochemical sensor for detecting lactic acid. The EEG electrode array includes a 6-channel recording electrode array with each electrode 30×50 μm in size, and the lactic acid sensor with overall contact is approximately 100 μm wide. The EEG electrodes have an average impedance of 2.57 kΩ at 1 kHz and remained stable after immersing in NS (normal saline) for 3 months. The lactic acid sensor showed a sensitivity of 52.8 nA mM^{-1}. The *in vivo* experiments demonstrated that the probe can reliably monitor electrophysiological signals. The probe is able to be implanted into the desired site with the help of a guide port. This flexible neural probe can provide more comprehensive insights into brain activity in the field of neuroscience and clinical practices.

1. Introduction

Acquisition and analysis of the brain's electroencephalogram (EEG) signal are critical for investigating essential life processes, aiding clinical diagnoses, and implementing disease surveillance.[1–8] It is well-documented that neural cells communicate with each other through electrical signals and chemical messengers,[9–16] and both of which are integrated into the function of neural circuits. Notably, neurological disorders, such as Parkinson's disease and schizophrenia, have been linked to atypical concentrations of various chemicals,[17–21] such as lactic acid. Researchers demonstrated that the level of lactic acid in the brain are linked to sleep, energy metabolism in the brain, and the formation of long-term memory.[22,23] Consequently, the simultaneous monitoring of electrical and chemical signals offers the opportunity both to investigate the relationship between these two types of signals and to enhance the accuracy of assessing brain activity levels.

Recent studies have introduced multimodal neural probes capable of concurrent electrical recording and neurotransmitter detection within the extracellular environment.[24–30] However, it is still a challenge to design a small-sized multimodal neural probe that can detect both neurotransmitters and neural signals. For multimodal neural probes, the large size of probe is necessary for attaining high-density neural recordings and high electrochemical sensitivity. The increase in the number of channels for monitoring electrophysiological signals directly correlates with the probe's width due to the linear relationship with the count of microelectrodes. Similarly, enhancing electrochemical detection's sensitivity and reliability requires the establishment of the three-electrode system by fabricating larger working electrodes (WEs) and incorporating two additional electrodes.[31] For implantable probes, the larger size will cause more severe damage to the brain tissue during implantation and generating more glial cells at the process of embedding, which adversely affect the long-term monitoring capabilities of the probe. Thus, striking a balance between the size and performance of probes represents a significant challenge in the development of small-sized multimodal neural probes.

In this work, we provided a multimodal integrated flexible neural probe with a small-sized design and employed a bifacial integration process that facilitates *in situ* recording of neural signals and the detection of lactic acid concentration simultaneously. Our development features a dual-sided integrated technique on a flexible substrate to minimize potential damage to brain tissue. Au microelectrodes were fabricated on one side of the neural probe, while 2 μm-thickness gold films were applied to decrease contact impedance. The average impedance of the microelectrode was approximately 2.57 kΩ at 1 kHz, maintaining stability after 3 months in normal saline, with impedance increasing by about 33%. On the opposite side of

The State Key Laboratory of Brain–Machine Intelligence, College of Information Science and Electronic Engineering, Zhejiang University, Hangzhou, 310027, China. E-mail: dongshurong@zju.edu.cn

the probe, lactic acid sensors with a size of around 100 μm were developed, leveraging the enzymatic catalysis of lactic acid by lactate oxidase in the presence of oxygen and modifying with Prussian blue to mitigate electrochemical interference,[32–34] achieving a sensitivity of 52.8 nA mM^{-1} for the lactic acid sensor. In addition, the entire head of the probe is equipped with a guide port, which allows the electrodes to be implanted into the desired site. The vivo experiments confirmed the probe's capability to monitor electrophysiological signals stably and consistently over extended periods.

2. Experimental

2.1 Materials and reagents

Acetic acid (CH$_3$COOH) and lactate oxidase were purchased from Macklin. Chitosan, H$_2$SO$_4$, KCl, HCl, acetone, isopropanol, PMMA, and phosphate buffer solution (PBS) were purchased from Sinopharm Chemical Reagent Co., China. Multi-walled carbon nanotubes were obtained from Suzhou Carbonfund Graphene Technology Co., China. FeCl$_3$·6H$_2$O, K$_3$Fe(CN)$_6$, lactic acid, HAuCl$_4$, and Nafion solution were purchased from Sigma-Aldrich. Allresist AR-P 5350 photoresist and Allresist AR 300-26 developer solution were purchased from Suzhou Research Material Micro–Nano Technology Co., China.

2.2 Fabrication of flexible multimodal integrated neural probe

The flexible multimodal integrated neural probe, depicted in Fig. 1, incorporates eight layers of materials across two main components. The front is a microelectrode array for monitoring neural electrical signals, the upper and lower encapsulation layer is PI, the middle electrode is Ti–Au–Ti, and 2 μm thickness gold films were applied to decrease contact impedance by chemical plating. The back side is the sensor for monitoring lactic acid content. The upper and lower encapsulation layer is PI, the intermediate electrode is Ti–Au–Ti, and the electrode contacts are modified with Au and plated with PB–lactate oxide–Nafion, and mixed with carbon nano-tubes to enhance its sensitivity. The two-sided integration process enables the neural probe to achieve more modes in a smaller size, reducing the tissue damage caused by implantation.

The glass sheet was ultrasonically cleaned with acetone, isopropanol, and deionized water, respectively, and dried after nitrogen blowing to obtain a clean and dry glass substrate. PMMA film was by spin-coating at 2000 rpm for 30 s and followed bake at 180 °C for 30 min to form a sacrificial layer. Spin-coat 60 s polyimide solution (thickness of about 15 μm) at 600 rpm, 105 °C for 30 min; 150 °C for 30 min; 180 °C for 30 min; 230 °C for 2 h, and use staged heating until it is cured. Spin-coat 60 s photoresist at 4000 rpm, and heat it at 105 °C for 4 min to obtain a photoresist of about 1 μm thickness, after a photolithography (MA6-BSA, Karl Suss, German) exposure of 1.7 seconds, the substrate was immersed in developer (developer: deionized water = 1 : 7) for 25 s. The substrate was cleaned by oxygen plasma for 5 min with a power of 140 W. A magnetron sputtering coating system (DISCOVERY-635, DENTON, USA) was used to sputter 10 nm of Ti, 600 nm of Au, and 10 nm of Ti to form a Ti–Au–Ti structure. After preparing the metal electrode layer, encapsulation was required. A 60 s polyimide solution (thickness of about 15 μm) was spin-coated at 600 rpm, 105 °C for 30 min; 150 °C for 30 min; 180 °C for 30 min; and 230 °C for 2 h, using staged heating until it cured. The photoresist covered the contacts and interfaces of the probes, and the photoresist was washed off after coating a 15 μm PMMA film. The sample was etched in an inductively coupled dry etching machine (Plasmapro100 Cobra 180, OXFORD, UK) for 25 min to expose the contacts and inter-faces and etch out the electrode profile. To enhance the stability and reliability of the electrodes in complex brain tissue, a commercial Pt electrode was set as the anode, and the electrode array was set as the cathode, they were then immersed into a mixture of 0.1 m HAuCl$_4$ and 1 m KCl with a current of 0.2 μA supplied by a digital source meter (Keithley 2400, Tektronix Inc.) for 40 s to obtain a layer of Au on the contacts and interfaces of electrode array. Finally, release the electrode array.
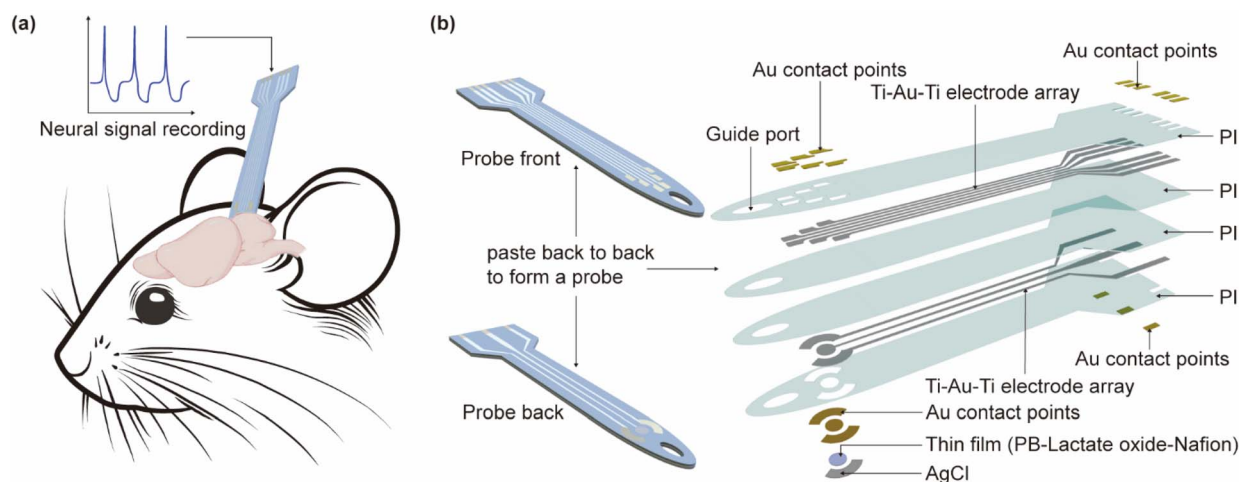

Fig. 1 The flexible multimodal integrated neural probe. (a) Diagram of the probe' functions; (b) diagram of the probe structure.

36% Acetic acid was diluted to 2%, and 20 mL was taken to completely dissolve 0.2 g of chitosan to obtain a 1 wt% chitosan solution. Then 40 mg of multi-walled carbon nanotubes were added to it and sonicated for 30 min to disperse uniformly to obtain a chitosan solution containing 2 mg mL^{-1} of multi-walled carbon nanotubes named solution 1. 100 U of lactate oxidase was dissolved in 50 μL of 100 mM of PBS buffer and sonicated for 30 min to obtain a uniformly dispersed lactate oxidase solution of concentration 2 U μL^{-1} named solution 2. 10 μL of solution 1 was mixed with 10 μL of solution 2 in equal volume and sonicated for 30 min to obtain a mixed solution of 1 U μL^{-1} of lactate oxidase.

Based on the mixed solution of ferric trichloride and potassium ferricyanide, the concentration of $FeCl_3$ in the solution is 2.5 mM L^{-1}, the concentration of $K_3Fe(CN)_6$ is 2.5 mM L^{-1}, and the concentration of KCl and HCl is 0.1 M L^{-1}. Prussian blue was prepared by reduction of potassium ferricyanide. The deposition potential is −0.5 V to about +0.4 V.

The lactic acid sensor preparation process was the same as that of the microelectrode. The reference electrode was coated with a layer of conductive silver ink and baked on a hot plate at 60 °C for 1 h. Then the whole electrode was added to 50 μL sulfuric acid solution (0.1 M L^{-1}), and the cyclic voltammetry (CHI760E, CH Instrument Co., USA), (1 V s^{-1} sweep speed, 10 turns) was scanned twice at 0.2–1.2 V to remove the impurities on the electrode surface meanwhile to activate the electrode. The AgCl referenced electrode was obtained by adding 50 μL $FeCl_3$ solution (0.1 M L^{-1}) to the electrode for the 20 s reaction. The electrode was washed 3 times with 0.1 M L^{-1} KCl/HCl mixture, and then 50 μL of Prussian blue solution was added to the electrode, and cyclic voltammetry was used to deposit Prussian blue onto the electrode surface. First, scan 2 cycles as a sweep speed of 20 mV s^{-1} under a voltage of −0.2 V–0.1 V, observe the position of the oxidation peak and reduction peak to adjust the scanning range, so that the cyclic voltammetry spectrum contains two complete peaks, and scan again so that the total number of times reaches 14 cycles. After scanning, the solution was dried to complete deposition. After completing the deposition of Prussian blue, 5 μL of lactate oxidase mixture was drop-coated on the working electrode and left to dry at room temperature, and 5 μL of 5 wt% Nafion solution was drop-coated on the working electrode and left to dry at room temperature to form a Nafion selective permeable membrane. The prepared lactic acid sensors were stored at 4 °C in a refrigerator.

The microelectrode array for monitoring electrical signals and the lactic acid sensors is pasted back-to-back to form
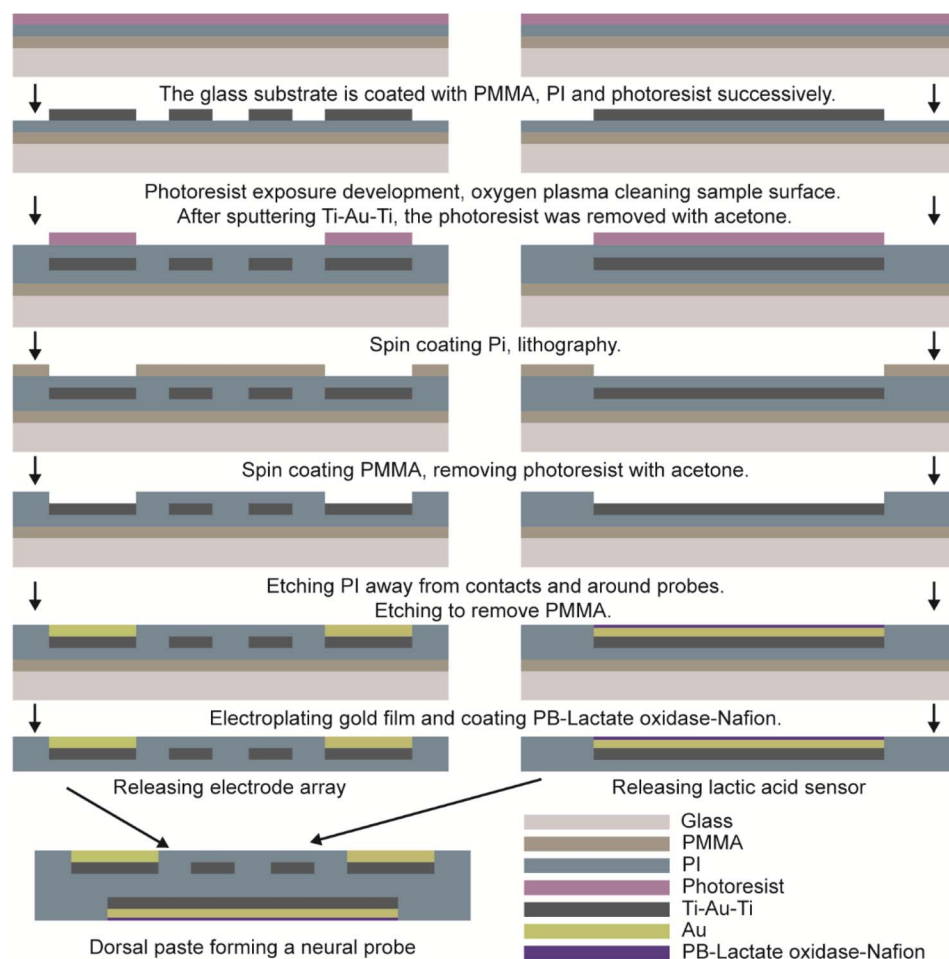

Fig. 2   The complete process flow.

a flexible double-sided multimodal integrated neural probe with a small size. The complete process flow is shown in Fig. 2.

2.3 *In vitro* experiment

The normal saline (NS) was used to simulate the humoral environment in the mice brain, and the impedance of the microelectrodes was tested in the frequency range of 0.1 Hz–10 kHz using the three-electrode system of the electrochemical workstation (CHI760E, CH Instrument Co., USA). The neural probe, Ag/AgCl, and graphene were employed as the working electrode, the referenced electrode, and the counter electrode, respectively. The physiological electrical signal sensing capability of microelectrode was characterized by an electrophysiological signal generator purchased from Blackrock (cereplex, USA), which could generate a simulated signal of local field potential (LFP) and spikes in NS.

Using a pipette gun, 50 μL of 100 mM PBS buffer was added to the electrode and scanned as the basal current, *i.e.*, the current at a lactic acid concentration of 0 mM L^{-1}, using the chronocurrent method. Subsequently, 1 μL of 51 mM, 157 mM, 214 mM, 326 mM, 389 mM, and 507 mM lactic acid solutions (all configured with PBS solution) were added to the electrode sequentially to detect lactic acid solutions of 0, 1, 4, 7, 10, 13, and 16 mM. The lactic acid solution was added each time to fully react with lactate oxidase, and then detected by the chronocurrent method, the current–time curve was recorded, and the sensitivity was analyzed based on the obtained data. A pipette was used to dispense 50 μL of 100 mM PBS buffer onto each of the four electrodes to establish the baseline current, defined as the current when the concentrations of glucose, ascorbic acid, glycine, and lactic acid were 0 mM L^{-1}. Scanning was then performed using the time–current method. Subsequently, solutions of 1 μL containing 51 mM lactic acid, 204 mM glucose, 51 mM ascorbic acid, and 51 mM glycine (all prepared in PBS) were sequentially added to the electrodes to detect 1 mM per L lactic acid, 4 mM per L glucose, 0.5 mM per L ascorbic acid, and 1 mM per L glycine. Each addition was allowed to fully react with lactate oxidase before chronocurrent detection.

2.4 *In vivo* experiment

The five mice used in the experiment were all male mice between 6 and 8 weeks of age and were allowed to acclimate in a standard animal room for at least 3 days before the experiment, during which they were fed standard amounts of food and water. All experiments conformed to the People's Republic of China Experimental Animal Management and Use Guidelines and the Guidelines for the Care and Use of Laboratory Animals of Zhejiang University. Additionally, all protocols were sanctioned by the Institutional Animal Care Committee. The mice were anesthetized by isoflurane, and the head was fixed to the stereotaxic apparatus (RWD, China). Head skin was incised to expose the skull with the appropriate hydrogen peroxide content and saline scrub. Then, a tiny craniotomy hole was made using a dental drill (RWD, China) for penicillin injection and probe implantation. Penicillin induces epileptic signals by blocking GABA_A receptors, reducing inhibitory neurotransmission in the brain, which leads to neuronal hyperexcitability and the uncontrolled firing of neurons, mimicking seizure-like activity. Epileptic foci were induced by injecting 500 IU penicillin (2 μl volume) into the right hippocampus (AP: −3.3 mm; ML: 2.2 mm; DV: −2.5 mm) using a microinjector. A neural probe was implanted at the injection site with a Pt wire for assistance, which was removed after implantation. This epileptic signal begins within 2–5 minutes of penicillin administration, lasts for 3–5 hours, and reaches a constant level of frequency and amplitude within 30 minutes.

3. Results and discussions

3.1 Probe structure

Fig. 3 is the fabricated flexible neural probe image, compared with a coin, demonstrating that the probe size is small enough to ensure its implantation into a mouse brain and does not interfere with its routine activities. Microscopic images of the probe are shown in the inset of Fig. 3, and it can be seen that the overall width of the probe is 115 μm, the oval implantation guide port at the front end is 50 μm, and the width of the microelectrode contact point is about 30 × 50 μm. The overall line profile of the microelectrode can also be seen in the microscopic image, which is very clear and indicates a high degree of reliability in the fabrication process. The inset shows the physical diagram of the lactic acid sensor, the overall size of the sensor electrode is about 100 μm, and the structure of the working electrode is the deposit of Prussian blue, lactate oxidase (chitosan, multi-walled carbon nanotubes) and Nafion on a gold film in sequence. In addition, a gold film was used as the counter electrode and AgCl was used as the referenced electrode.

3.2 *In vitro* characterization of microelectrodes of fabricated neural probe

The impedance scanning of the microelectrodes was performed in NS, and the results are shown in Fig. 4a, which shows the impedance spectra of each of the 6 channels at 1 Hz–10 kHz. The difference between the impedance values of each channel is not obvious, with multi-channel consistency, and the slight difference may be caused by the difference in the size of the contact point. As can be seen from Fig. 4b, when the scanning frequency is at 1 kHz, the impedance of each channel of the probe is less than 2.85 kΩ, and its average impedance is about 2.57 kΩ (std: 0.14 kΩ), which meets the requirements of electrophysiological signal detection.[35] Fig. 4c and d respectively show the electrophysiological analog signal and signal power spectrum collected by the microelectrode, which are generated by the electrophysiological signal generator. It can be seen that the signal consistency of the 6-channel microelectrode in the flexible neural probe is strong, and the acquisition frequency distribution of each channel is also consistent. The neural probe was bent (bending radius of ∼0.3 cm) 100, 200, 500, and 1000 times to measure its impedance at 1 kHz to verify its flexibility. Fig. 4e shows that the impedance value of the 6-channel electrode increases by less than 10% at 1 kHz after
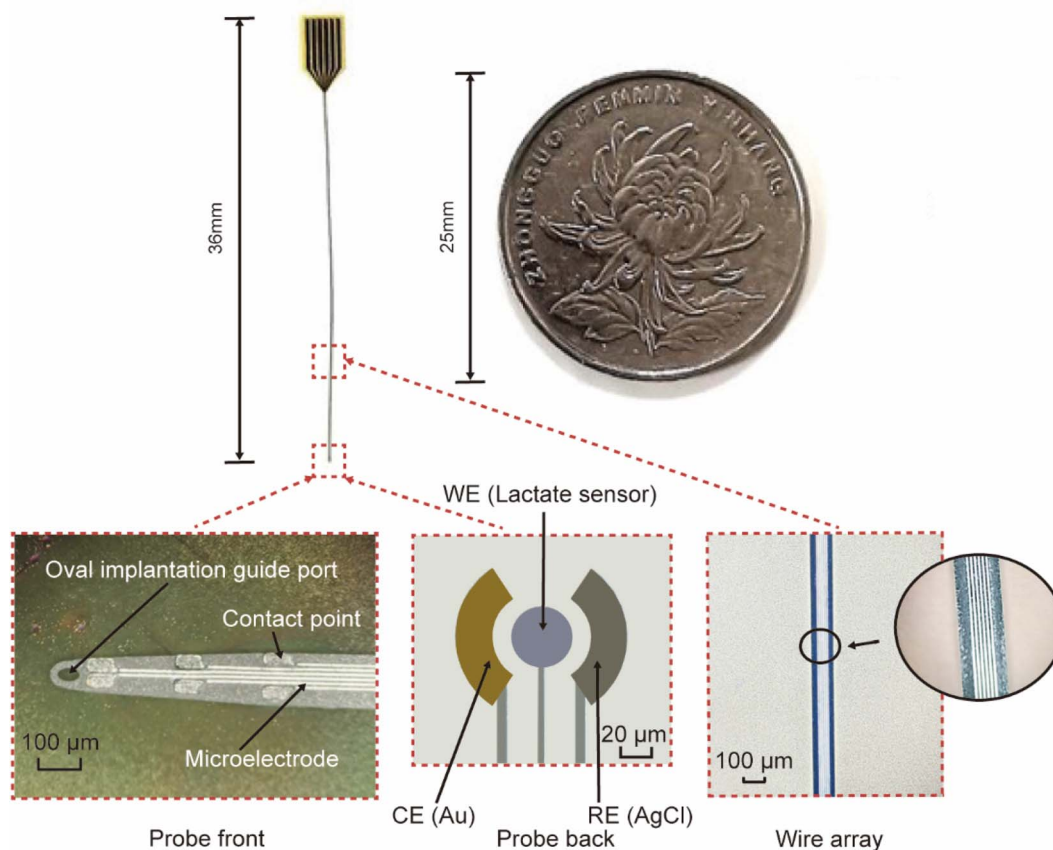
Fig. 3 The size comparison of a flexible neural probe and a coin, inset: probe front, probe back, and wire array, respectively.

bending 1000 times. The flexible neural probe was infiltrated in NS to verify its stability. As shown in Fig. 4f and g, the probe can be stable in the NS environment for more than 3 months, with only a 33.3% increase in impedance compared to before infiltration. The micrograph of the probe after infiltration is shown in the inset of Fig. 4g, which clearly shows that the microelectrode lines are still clear and stable.

3.3 *In vitro* characterization of lactic acid sensor of fabricated neural probe

Prussian blue (PB) is a catalyst used to reduce hydrogen peroxide and oxygen.[32] The reduction of hydrogen peroxide in the bare gold electrode requires a high potential, and there are usually a lot of electroactive substances in this range, which will produce a lot of interference signals to the sensor. After the Prussian blue modification, it has good selectivity for hydrogen peroxide, and can easily detect hydrogen peroxide at low potential to reduce electrochemical interference.[33,36,37] The reaction between lactate oxidase and lactic acid produces pyruvate and hydrogen peroxide. When a positive voltage is applied to the electrode to oxidize hydrogen peroxide, oxygen, hydrogen ions, and electrons are generated, and the electrons form a detecting current through the electrode loop, and its size is proportional to the concentration of lactic acid. As shown in Fig. 5a, the response curves of lactic acid concentration of 0, 1, 4, 7, 10, 13, and 16 mM, respectively. The standard response

curve of lactic acid concentration is shown in Fig. 5b. It can be seen that the electrode modification scheme is effective and the linearity is good. The lactic acid sensor has a sensitivity of 52.8 nA mM^{-1} (2.33 μA mM^{-1} cm^{-2}) and a correlation coefficient of 0.9925. Compared with existing sensors for lactic acid detection (sensitivity 0.256 μA mM^{-1} cm^{-2}), the lactic acid sensor prepared in this study is not only smaller but also about 9 times more sensitive.[38]

In the actual cerebrospinal fluid environment, many other compounds besides lactic acid may interfere with sensor recognition. For example, compounds such as glucose, ascorbic acid, and glycine are common components of cerebrospinal fluid. To verify the anti-interference ability of the lactic acid sensor prepared in this study, it is necessary to compare the response currents of the lactic acid sensor for these compounds and lactic acid. The response currents were 5.3, 49.7, 4.1, and 1188.3 nA for glucose (4 mM L^{-1}), ascorbic acid (0.5 mM L^{-1}), glycine (1 mM L^{-1}), and lactic acid (1 mM L^{-1}), respectively. As shown in Fig. 5c, the response currents of the interfering compounds were negligible compared to those of lactic acid.

3.4 *In vivo* characterization of flexible multimodal integrated neural probe

To evaluate the carrier's ability of the flexible neural probe, we evoked epileptic signals in the right hippocampus of mice and recorded them in real-time. We evoked epileptic signals in mice
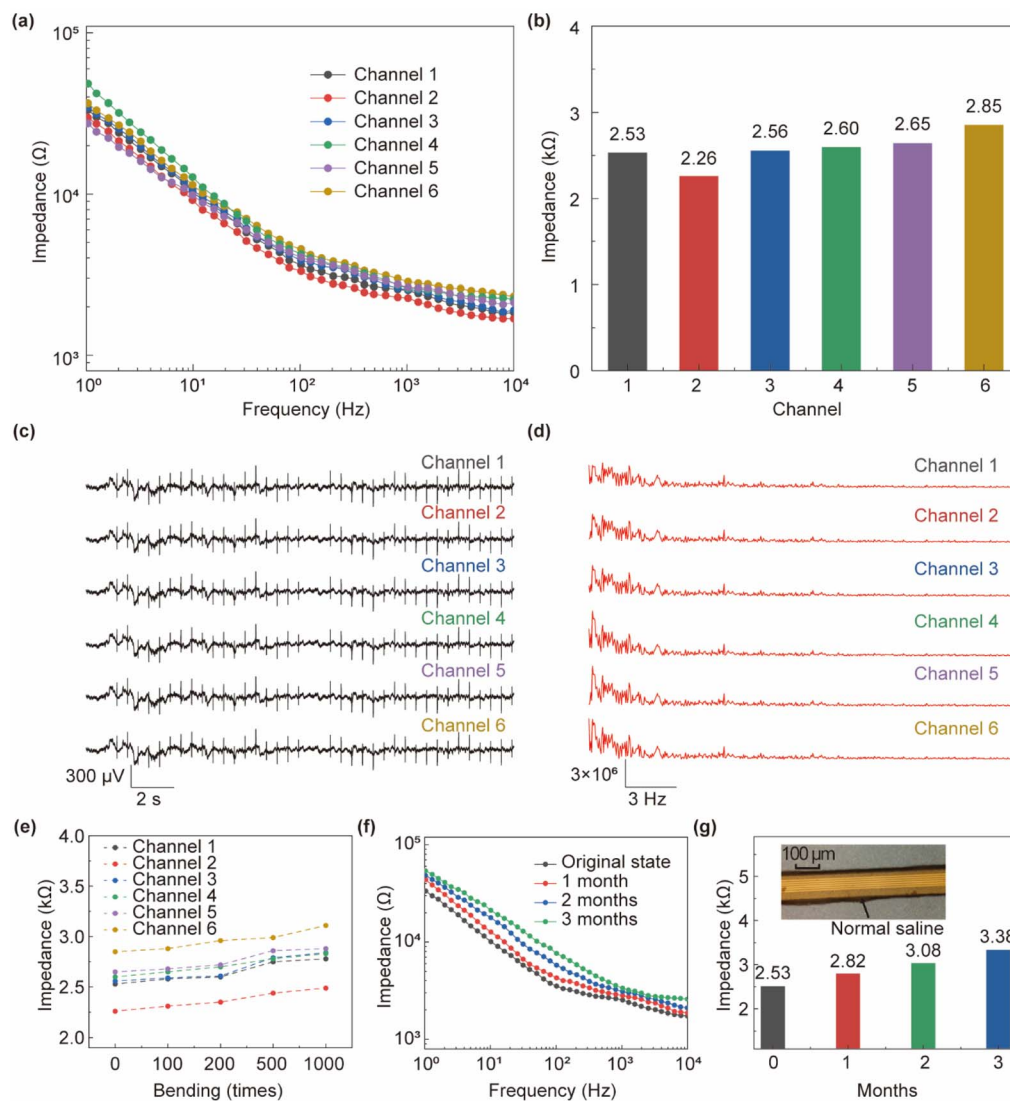
Fig. 4 (a) The impedance spectrum of a 6-channel microelectrode; (b) the impedance value of a 6-channel microelectrode at 1 kHz; (c) the electrophysiological signals collected by a 6-channel microelectrode *in vitro*; (d) the power spectrum collected by a 6-channel microelectrode *in vitro*; (e) the flexibility of neural probe (100, 200, 500 and 1000 times respectively); (f) the stability of flexible neural probe (1, 2 and 3 months respectively); (g) the micrograph of a flexible neural probe after 3 months of NS infiltration.
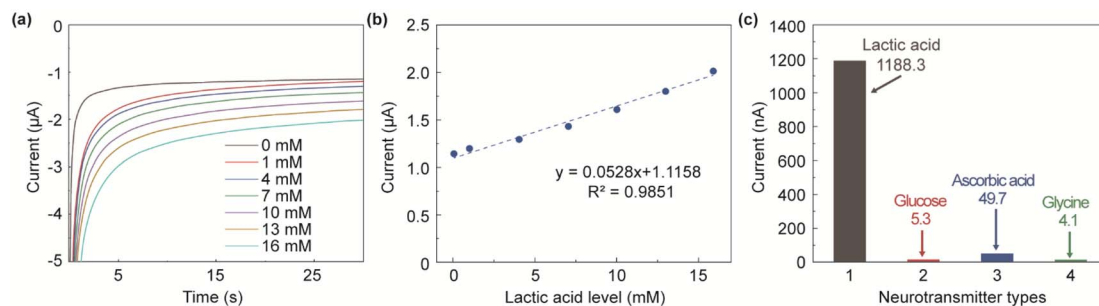

Fig. 5 (a) The lactic acid concentration response curve; (b) the standard response curve of lactic acid concentration; (c) the infectivity test of lactic acid sensor.
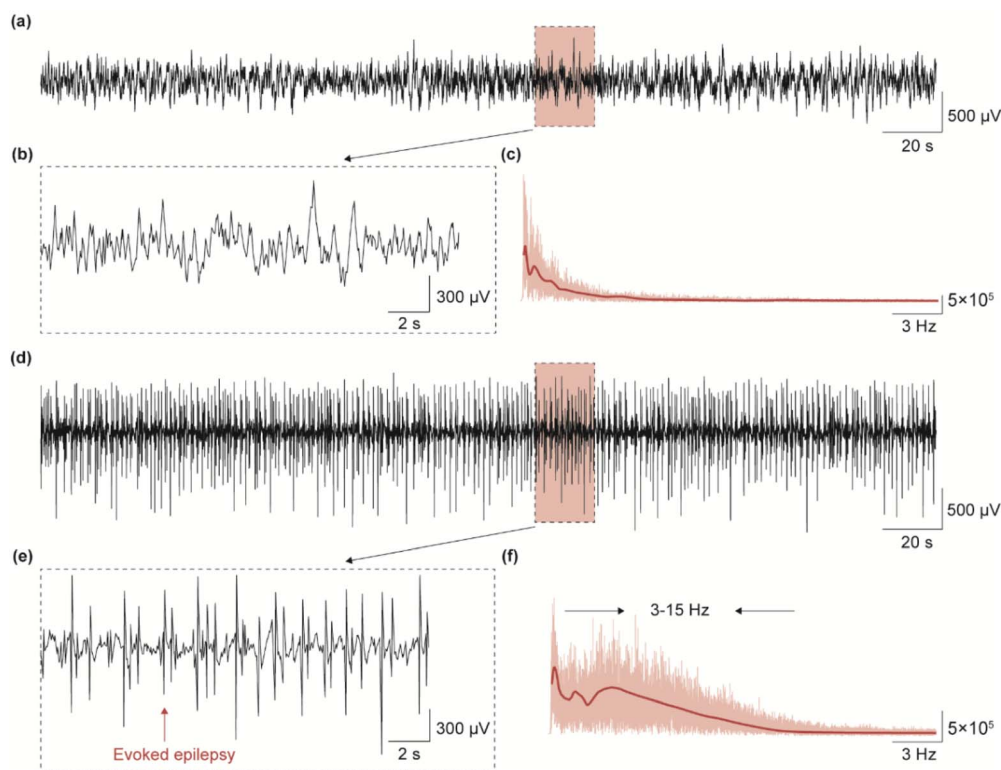
Fig. 6 (a) The neural signals that precede evoked epilepsy (300 s); (b) the 20 s local neural signals in (a); (c) the power spectrum of signals precedes evoked epilepsy; (d) the neural signals that after evoked epilepsy (300 s); (e) the 20 s local neural signals in (d); (f) the power spectrum of signals after evoked epilepsy.

Table 1 Comparison with reported flexible neural probe

Reference	Materials	Impedance at 1 kHz	Electrode size	Multi-modal
This work	PI/Au/Ti	∼2.57 kΩ	115 μm	Yes
1 (ref. 39)	PI/Parylene C/Si/PtNM	643(±208) kΩ	10 μm	No
2 (ref. 40)	PEDOT: PSS/IrOx	36.97(±4.68)–56.46(±7.10) kΩ	14 × 24 μm2	No
3 (ref. 41)	Hydrogel/PEI/PC/COC/Sn	≈1 MΩ	100 μm in diameter	Yes
4 (ref. 42)	Porous Pt	∼30 kΩ	50 μm	No
5 (ref. 43)	TiN	∼10 kΩ	4 × 4 mm^2	No
7 (ref. 44)	Si	∼1 MΩ	60 μm	No
8 (ref. 45)	PI/Au/Cr	∼2.6 MΩ	200 μm	Yes
9 (ref. 46)	PI/Al/Cr/Ti/Pt	∼650 kΩ	4000 μm	Yes

by injecting appropriate amounts of penicillin and compared the changes in neural signals before and after. Fig. 6a shows the LFP signals of anesthetized mice at 300 s when their brains were functioning normally, and Fig. 6b shows a local magnification of the LFP signals in Fig. 6a (20 s). In this case, no abnormal discharge signal was found in the LFP signal of the mice. Fig. 6c shows the power spectrum of the pre-evoked signal, and it can be seen that the signal is mainly distributed in the range of 1–3 Hz. Fig. 6d shows the LFP signal at 300 s during evoked epileptic in the brain of an anesthetized mouse, and Fig. 6e shows an amplified 20 s epileptic LFP signal, which shows a strong abnormal epileptic spike. The power spectrum analysis in Fig. 6f shows that the distribution region of the LFP signal in the epileptic state widens to the right and is mainly concentrated between 1 and 15 Hz. The results in Fig. 6 show that the

flexible neural probe we prepared is capable of acquiring high-quality LFP signals in organisms and for epilepsy monitoring.

3.5 Summary of materials, and characteristics of flexible neural probe

In comparison with conventional implantable neural probes, as shown in Table 1, our neural probe has multimodal and better electric characteristics, while the small size causes little damage to brain tissue.

4. Conclusions

The creation of small-sized neural probes capable of simultaneously monitoring electrical signals and chemical substances

presents a significant challenge, primarily due to the trade-off between the probe's size and its performance. This paper developed a method to construct an efficient dual-sided flexible multimodal integrated neural probe. This design incorporates a 6-channel microelectrode array alongside a lactic acid sensor. The microelectrode demonstrated an average impedance of approximately 2.57 kΩ at 1 kHz, maintaining stability after 3 months in normal saline with a modest increase in impedance of about 33%. The lactic acid sensor on the other side of the probe is based on the principle that lactate oxidase catalyzes lactic acid to generate hydrogen peroxide and uses PB modified electrode to measure the reaction current, obtaining a sensitivity of 52.8 nA mM^{-1}. This sensitivity is consistent with the range of lactic acid in the human body. In addition, the entire head of the probe is equipped with guide holes, facilitating precise electrode implantation into the target site using a microscope, a guide needle, or other implantation tools. Finally, the vivo experiments confirmed that the neural probe was able to stably monitor electrophysiological signals and detect epileptic bursts in real-time.

In conclusion, our neural probe demonstrates superior performance. In future studies, we aim to further enhance the electrical performance of the electrode arrays, improve the sensitivity of the lactate sensor, and optimize the biological model. These advancements are expected to facilitate the application of our multimodal neural probe for *in situ*, real-time monitoring in both clinical and basic neurotechnology research.

Data availability

The data presented in this study are available on request from the corresponding author. The data are not publicly available due to privacy.

Author contributions

Conceptualization, S. D. and L. Z.; methodology, L. Z. and Z. C.; validation, L. Z.; investigation, J. X.; data curation, L. Z. and B. L.; writing—original draft preparation, L. Z.; writing—review and editing, S. D., L. Z. and Z. C.; supervision, J. X.; project administration, L. Z. and Z. C. All authors have read and agreed to the published version of the manuscript.

Conflicts of interest

The authors declare that they have no known competing financial interests or personal relationships that could have appeared to influence the work reported in this paper.

Acknowledgements

Notes and references

1 G. Kook, S. W. Lee, H. C. Lee, I.-J. Cho and H. J. Lee, *Micromachines*, 2016, **7**, 179.
2 S. Siuly, Y. Li and Y. Zhang, *IEEE Trans. Neural Syst. Rehabil. Eng.*, 2016, **11**, 141–144.
3 D. Khodagholy, J. N. Gelinas, T. Thesen, W. Doyle, O. Devinsky, G. G. Malliaras and G. Buzsáki, *Nat. Neurosci.*, 2015, **18**, 310–315.
4 P. Shirvalkar, J. Prosky, G. Chin, P. Ahmadipour, O. G. Sani, M. Desai, A. Schmitgen, H. Dawes, M. M. Shanechi and P. A. Starr, *Nat. Neurosci.*, 2023, **26**, 1090–1099.
5 L. Q. Uddin, *Nat. Rev. Neurosci.*, 2021, **22**, 167–179.
6 A. Ing, P. G. Sämann, C. Chu, N. Tay, F. Biondo, G. Robert, T. Jia, T. Wolfers, S. Desrivières and T. Banaschewski, *Nat. Human Behav.*, 2019, **3**, 1306–1318.
7 S. Wang, Q. Jiang, H. Liu, C. Yu, P. Li, G. Pan, K. Xu, R. Xiao, Y. Hao and C. Wang, *Proc. Natl. Acad. Sci. U.S.A.*, 2024, **121**, e2403380121.
8 X. Cai, H. Zhang, P. Wei, Q. Liu, D. Sheng, Z. Li, B. Zhang, G. Tang, W. Zhao and Z. Ye, *Nat. Photonics*, 2024, 1–9.
9 A. B. Schwartz, *Annu. Rev. Neurosci.*, 2004, **27**, 487–507.
10 J. A. Frank, M.-J. Antonini and P. Anikeeva, *Nat. Biotechnol.*, 2019, **37**, 1013–1023.
11 M. Lee, H. J. Shim, C. Choi and D.-H. Kim, *Nano Lett.*, 2019, **19**, 2741–2749.
12 J. Scholz and C. J. J. N. n. Woolf, *Nat. Neurosci.*, 2007, **10**, 1361–1368.
13 J. A. Filosa, A. D. Bonev, S. V. Straub, A. L. Meredith, M. K. Wilkerson, R. W. Aldrich and M. T. Nelson, *Nat. Neurosci.*, 2006, **9**, 1397–1403.
14 E. T. Kavalali, *Nat. Rev. Neurosci.*, 2015, **16**, 5–16.
15 T. Branco and K. Staras, *Nat. Rev. Neurosci.*, 2009, **10**, 373–383.
16 J.-P. Changeux, *Sci. Am.*, 1993, **269**, 58–62.
17 A. Baranwal and P. Chandra, *Biosens. Bioelectron.*, 2018, **121**, 137–152.
18 Z. R. Donaldson and L. Young, *Science*, 2008, **322**, 900–904.
19 W. C. Drevets, J. L. Price and M. L. Furey, *Brain Struct. Funct.*, 2008, **213**, 93–118.
20 B. S. Meldrum, *J. Nutr.*, 2000, **130**, 1007S–1015S.
21 H. Wei, L. Li, J. Jin, F. Wu, P. Yu, F. Ma and L. Mao, *Anal. Chem.*, 2020, **92**, 10177–10182.
22 E. Naylor, D. V. Aillon, B. S. Barrett, G. S. Wilson, D. A. Johnson, D. A. Johnson, H. P. Harmon, S. Gabbert and P. A. Petillo, *Sleep*, 2012, **35**, 1209–1222.
23 A. Suzuki, S. A. Stern, O. Bozdagi, G. W. Huntley, R. H. Walker, P. J. Magistretti and C. M. Alberini, *Cell*, 2011, **144**, 810–823.
24 M. Johnson, R. Franklin, K. Scott, R. Brown and D. Kipke, *IEEE Engineering in Medicine & Biology Conference*, 2006, pp. 7325–7328.
25 U. Chae, H. Shin, N. Choi, M.-J. Ji, H.-M. Park, S. H. Lee, J. Woo, Y. Cho, K. Kim and S. Yang, *Biosens. Bioelectron.*, 2021, **191**, 113473.

26 U. Chae, J. Woo, Y. Cho, J.-K. Han, S. H. Yang, E. Yang, H. Shin, H. Kim, H.-Y. Yu and C. Lee, *Proc. Natl. Acad. Sci. U. S. A.*, 2023, **120**, e2219231120.

27 S. Nimbalkar, E. Castagnola, A. Balasubramani, A. Scarpellini, S. Samejima, A. Khorasani, A. Boissenin, S. Thongpang, C. Moritz and S. Kassegne, *Sci. Rep.*, 2018, **8**, 6958.

28 B. Fan, C. A. Rusinek, C. H. Thompson, M. Setien, Y. Guo, R. Rechenberg, Y. Gong, A. J. Weber, M. F. Becker and E. Purcell, *Microsyst. Nanoeng.*, 2020, **6**, 42.

29 G. Xiao, Y. Song, Y. Zhang, Y. Xing, H. Zhao, J. Xie, S. Xu, F. Gao, M. Wang and G. Xing, *ACS Sens.*, 2019, **4**, 1992–2000.

30 S. Zhang, Y. Song, M. Wang, G. Xiao, F. Gao, Z. Li, G. Tao, P. Zhuang, F. Yue and P. Chan, *Microsyst. Nanoeng.*, 2018, **4**, 1–9.

31 L. Ianeselli, G. Grenci, C. Callegari, M. Tormen and L. Casalis, *Biosens. Bioelectron.*, 2014, **55**, 1–6.

32 K. Itaya, N. Shoji and I. J. Uchida, *J. Am. Chem. Soc.*, 1984, **106**, 3423–3429.

33 A. A. Karyakin, O. V. Gitelmacher and E. E. Karyakina, *Anal. Lett.*, 1994, **27**, 2861–2869.

34 W. Gao, S. Emaminejad, H. Y. Y. Nyein, S. Challa, K. Chen, A. Peck, H. M. Fahad, H. Ota, H. Shiraki and D. Kiriya, *Nature*, 2016, **529**, 509–514.

35 D.-W. Park, A. A. Schendel, S. Mikael, S. K. Brodnick, T. J. Richner, J. P. Ness, M. R. Hayat, F. Atry, S. T. Frye and R. Pashaie, *Nat. Commun.*, 2014, **5**, 5258.

36 H. Song, H. Shin, H. Seo, W. Park, B. J. Joo, J. Kim, J. Kim, H. K. Kim, J. Kim and J. U. Park, *Adv. Sci.*, 2022, **9**, 2203597.

37 W. Park, H. Seo, J. Kim, Y.-M. Hong, H. Song, B. J. Joo, S. Kim, E. Kim, C.-G. Yae and J. Kim, *Nat. Commun.*, 2024, **15**, 2828.

38 R. Garjonyte, Y. Yigzaw, R. Meskys, A. Malinauskas and L. Gorton, *Sens. Actuators, B*, 2001, **79**, 33–38.

39 S. H. Lee, M. Thunemann, K. Lee, D. R. Cleary, K. J. Tonsfeldt, H. Oh, F. Azzazy, Y. Tchoe, A. M. Bourhis and L. Hossain, *Adv. Funct. Mater.*, 2022, **32**, 2112045.

40 E. J. Musk, *J. Med. Internet Res.*, 2019, **21**, e16194.

41 S. Park, H. Yuk, R. Zhao, Y. S. Yim, E. W. Woldeghebriel, J. Kang, A. Canales, Y. Fink, G. B. Choi and X. Zhao, *Nat. Commun.*, 2021, **12**, 3435.

42 M. Leber, R. Bhandari, J. Mize, D. Warren, M. Shandhi, F. Solzbacher and S. Negi, *Biomed. Microdevices*, 2017, **19**, 1–12.

43 J. D. Weiland, D. J. Anderson and M. S. Humayun, *IEEE Trans. Biomed. Eng.*, 2002, **49**, 1574–1579.

44 D. R. Kipke, R. J. Vetter, J. C. Williams and J. F. Hetke, *IEEE Trans. Neural Syst. Rehabil. Eng.*, 2003, **11**, 151–155.

45 H.-Y. Lai, L.-D. Liao, C.-T. Lin, J.-H. Hsu, X. He, Y.-Y. Chen, J.-Y. Chang, H.-F. Chen, S. Tsang and Y.-Y. I. Shih, *J. Neural. Eng.*, 2012, **9**, 036001.

46 S. Metz, A. Bertsch, D. Bertrand and P. Renaud, *Biosens. Bioelectron.*, 2004, **19**, 1309–1318.